IEEE Access
Multidisciplinary ⋮ Rapid Review ⋮ Open Access Journal

Received 6 June 2023, accepted 6 August 2023, date of publication 15 August 2023, date of current version 7 September 2023.

Digital Object Identifier 10.1109/ACCESS.2023.3305434

RESEARCH ARTICLE

Analysis of Slipper Overturning and Collision Behavior of the Axial Piston Pump Based on Rigid-Flexible Coupling

LIRONG WAN, JINYING JIANG, ZHIYUAN SUN, AND HAO NIU
College of Mechanical and Electronic Engineering, Shandong University of Science and Technology, Qingdao 266590, China
Corresponding author: Zhiyuan Sun (zysun@sdust.edu.cn)

This work was supported in part by the National Natural Science Foundation of China under Grant 52274132.

ABSTRACT In the working process of the axial piston pump, the composite multi-degree motion of the slipper and its coupling, as well as the complex working conditions, cause the slipper to overturn and collide irregularly with its coupling. The overturning of the slipper leads to partial abrasion of the slipper, and the magnitude of the force generated by direct solid contact between the slipper and the swash plate significantly impacts the wear speed of the slipper. This article is based on the rigid-flexible coupling model of the axial piston pump jointly established by Adams and Ansys. It analyzes the collision relationship between the slipper and its coupling, the overturning behavior characteristics of the slipper, and the variation law in the overturning and collision behavior of the slipper under different spring forces and load pressure, besides, the correlation analysis of the result data is conducted through multiple linear regression method. The research results indicate that the overturning and collision behavior of the slipper exhibits a certain periodicity. Appropriate spring preload and piston chamber oil pressure can effectively reduce the overturning degree of the slipper, reduce the collision strength between the slipper and its coupling, and thus reduce the partial abrasion of the slipper. The research results of this article provide a reference for the wear failure analysis and structural optimization of the slipper.

INDEX TERMS Slipper, overturning, collision, partial abrasion.

I. INTRODUCTION

With the development of hydraulic technology, piston pumps are widely used in fields [1] such as engineering machinery, mining metallurgy, and agricultural machinery due to their compact structure, high power density, and convenient variable control [2], [3]. The axial piston pump is a typical positive-displacement hydraulic machine that relies on the relative motion of various internal components [4], [5] to complete the flow distribution action. Its high-pressure and high-speed operation [6], [7] is beneficial for improving volumetric efficiency, but it also leads to poor internal friction conditions [8], through analysis of the causes of the piston pump failure, it was found that the wear problem of the slipper and swash plate is one of the main factors causing the piston pump failure, especially the slipper, as the most complex motion mechanism and the harshest working environment component [9], is prone to overturning behavior, and it had a strong collision with its coupling [10] which led to the failure of the slipper to form a stable oil film lubrication. The partially mixed friction or even dry friction of the slipper/swash plate interface increased energy consumption, and the energy consumption turned into heat [9], reducing the oil viscosity, weakening the bearing capacity of the oil film, leading to partial abrasion of the slipper [11], which seriously affected the mechanical efficiency and volumetric efficiency of the whole pump, and even led to the failure of the piston pump [12].

To study the cause of wear failure of slippers, Zhang et al. [13] designed a new type of slipper rotation testing device, and the measurement results showed that the slipper follows the piston and cylinder block in reciprocating circumferential

The associate editor coordinating the review of this manuscript and approving it for publication was Hassen Ouakad.

and axial motion at the macro level, while at the micro level, there is spin motion, squeezing motion, and overturning motion; Ransegnola et al. [14] studied the spin behavior of slippers and pistons by establishing a fully coupled model; Zhou et al. [15] designed a dynamic lubrication performance testing platform for slippers, which is used to measure the working attitude of slippers in real time under actual working conditions; Xu et al. [16] established a numerical model of the slipper pair based on the theory of elastohydrodynamic mechanics, and studied the micromotion and pressure distribution of the slipper. The study pointed out that the overturning behavior of the slipper is the main cause of partial abrasion of the slipper; Chao et al. [17] pointed out that the collision and direct solid contact between the slipper and the swash plate are important factors causing the wear of the slipper; Jiang and Wang [18] pointed out that the overturning and partial abrasion of the slipper increases the frictional power loss of the piston pump, and the micro-chamfering structure of the slippers helps to increase the oil film thickness, reduce direct solid contact and collision between the slipper and swash plate; Meng et al. [19] and Ozmen [20] proposed that as the rotational speed increases, the oil film thickness of the slipper pair decreases. Avoiding direct solid contact between the slipper and the swash plate is of great significance in reducing slipper wear; Shorbagy et al. [21] found that the characteristics of lubricating oil films largely depend on the micromotion and elastic deformation of rotating components; Tang et al. [22], [23] established a mathematical model of oil film thickness and a thermos-elastohydrodynamic lubrication model for the slipper/swash plate interface of axial piston pump based on considering the thermal effect of the oil. The study found that the piston chamber oil pressure and speed have a certain impact on the overturning behavior and leakage amount of the slipper, and the performance of the slipper can be improved by optimizing the structure of the slipper.

In terms of the dynamic relationship between the slipper and its coupling, Wang et al. [24] proposed that there is serious collision interference between the neck of the slipper and the slipper retainer, and the collision intensity increases with the increase of the swash plate angle and pump shaft speed; Haidak et al. [25] studied the deformation and fracture mechanism of the slipper retainer and proposed solutions for the structural dimensions and materials of the slipper retainer to ensure its service life; Hu et al. [26] introduced the body coordinate system of the piston pump and established a precise mathematical model of the slipper-piston component to achieve dynamic evaluation of the dynamic performance of the slipper-piston component throughout the entire cycle; Decken and Murrenhoff [27] established a virtual prototype of piston pump through ADAMS and self-designed hydraulic system software DSHplus and studied the complex interaction between contact friction, dynamics, and kinematics of pump components. Shen et al. [28] established a virtual prototype of a piston pump and comprehensively analyzed the effects of the piston chamber oil pressure, piston radius, and radial clearance on the contact force of the slipper/piston; Yang et al. [29] simulated and analyzed the stress and temperature distribution of the slipper and piston in view of the problems that are easy to occur in the severe working conditions of the aviation hydraulic pump; Yao et al. [30] analyzed the stress and strain generated by the slipper and piston during the crimping process using finite element software Ansys.

To sum up, the existing research on the overturning behavior of the slipper focuses on the distribution of the oil film thickness of the slipper pair, and mostly uses the simplified numerical model for analysis. It cannot reflect the impact of the slipper's coupling on the kinematics and dynamic behavior of the slipper in the whole movement cycle. However, the overturning behavior of the slipper and the collision behavior of the slipper and its coupling have an important impact on the partial abrasion of the slipper. In addition, there is a lack of research on the real-time stress and deformation of the slipper under the conditions of overturning and collision behavior. Therefore, this article studies the dynamic characteristics of slipper overturning and collision behavior based on the rigid-flexible coupling model of the piston pump, discusses the effects of the spring preload and piston chamber oil pressure on slipper overturning and collision behavior, and analyzes the correlation of the results data through multiple linear regression method. At the same time, real-time stress and deformation of the slipper are observed. To achieve the goal of reducing wear, improving lubrication, and increasing the service life of piston pumps.

II. DYNAMIC MODEL OF AXIAL PISTON PUMP

A. HERTZ CONTACT MODEL

There are two calculation methods for contact force in Adams. One is to calculate the contact force through penalty parameters and regression coefficients, and the other is the collision function contact algorithm based on Hertz contact theory. In this article, the contact force between the slipper and the swash plate, as well as the contact force between the slipper and the slipper retainer, are solved using the impact method based on Hertz contact theory. The Hertz contact force can be expressed as:

$$F_{Her} = K\delta^n + K\delta^n D_n \dot{\delta} \tag{1}$$

$$K = \frac{4\sqrt{R}}{3}E \tag{2}$$

$$E = \frac{1-\mu_1^2}{E_1} + \frac{\mu_2^2}{E_2} \tag{3}$$

where F_{Her} is the Hertz contact force, δ is the contact deformation, K is the contact stiffness, D_n is the damping coefficient, R is the equivalent radius, E is the equivalent elastic modulus, E_1, E_2, μ_1, μ_2 represents the elastic modulus and Poisson's ratio of the two contact bodies.

B. MATHEMATICAL MODEL OF THE SLIPPER/SWASH PLATE INTERFACE

The piston pump is a power component that converts mechanical energy into hydraulic energy through mechanical motion.

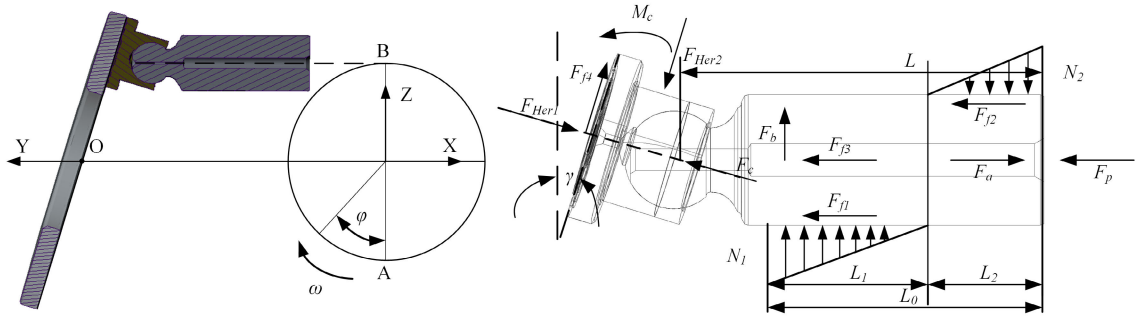

FIGURE 1. Kinematics and dynamics analysis of slipper pair.

The prime mover is connected to the drive shaft of the piston pump, which drives the cylinder block to rotate, and the slipper-piston follows the cylinder block in circumferential motion; At the same time, under the combined action of high-pressure oil and slipper retainer, the slipper-piston completes the reciprocating axial motion in the hole of the cylinder block, and ultimately the piston pump completes periodic oil suction and discharge actions through this composite motion.

Fig. 1 shows the kinematics and dynamics analysis of the slipper-piston. In Fig. 1, R is the radius of the cylinder block distribution circle, γ is the inclination angle of the swash plate, ω is the speed of the drive shaft. When the slipper-piston is located at point A, the piston extends the longest length in the cylinder block. When the piston moves from point A to point B, the angle is φ, and the displacement of the slipper-piston relative to the origin O in all directions is:

$$\begin{cases} x = -Rsin\varphi = -Rsin\omega t \\ z = -Rcos\varphi = -Rcos\omega t \\ y = Rtan\Upsilon cos\varphi = Rtan\Upsilon cos\omega t \end{cases} \tag{4}$$

Equation (4) takes the derivative of time to obtain the velocities of the slipper-piston relative to point O in all directions:

$$\begin{cases} v_x = \dot{x} = -\omega Rcos\omega t \\ v_z = \dot{z} = \omega Rsin\omega t \\ v_y = \dot{y} = -\omega Rtan\Upsilon sin\omega t \end{cases} \tag{5}$$

The acceleration of the slipper-piston relative to the O point in each direction can be obtained by taking second derivative of Equation (4):

$$\begin{cases} a_x = \ddot{x} = \omega^2 Rsin\omega t \\ a_z = \ddot{z} = \omega^2 Rcos\omega t \\ a_y = \ddot{y} = -\omega^2 Rtan\Upsilon cos\omega t \end{cases} \tag{6}$$

The piston pump often operates under high-speed and high-pressure conditions, and each component bears a large load. The slipper-piston is the core working component in the piston pump, so it is necessary to conduct a dynamic analysis on it.

The oil pressure F_p in the piston chamber is:

$$F_p = \frac{\pi d^2}{4} P \tag{7}$$

where d is the diameter of the piston and P is the piston chamber oil pressure.

The axial inertia force F_a of the piston group is:

$$F_a = (m_1 + m_2) R\omega^2 tan\Upsilon cos\varphi \tag{8}$$

where m_1 is the mass of a single piston, and m_2 is the mass of a single slipper.

The centrifugal force F_b generated by the circumferential movement of the piston group is:

$$F_b = (m_1 + m_2) R\omega^2 \tag{9}$$

The centrifugal force generated during the circumferential movement of the piston group with the cylinder block causes the piston to tilt in the cylinder block, causing contact of the piston/inner wall of the cylinder block and generating upper support reaction force N_1 and lower support reaction force N_2. The relationship between N_1 and N_2 can be expressed as:

$$\begin{cases} N_1 L_2^2 = N_2 L_1^2 \\ N_1 \left[3 \left(L - L_0\right) + L_1\right] = N_2 \left(3L - L_2\right) \end{cases} \tag{10}$$

where L is the length of the piston, and L_0 is the fitting length between the piston and the hole of the cylinder block when the piston is at its longest extension.

Due to the presence of upper and lower reaction forces between the piston and the inner wall of the cylinder block, as well as the relative axial movement between the piston and the cylinder block, frictional forces F_{f1}, F_{f2}, and total frictional force F_{f3} are generated, which can be expressed as:

$$F_{f3} = F_{f1} + F_{f2} = sgn\,(v) f_1 (N_1 + N_2) \tag{11}$$

where f_1 is the friction coefficient between the piston and the cylinder block.

There is contact force F_{Her1} and friction force F_{f4} between the slipper and the swash plate. The friction force F_{f4} between the slipper and the swash plate is:

$$F_{f4} = F_{Her1} f_2 \tag{12}$$

where f_2 is the friction coefficient between the swash plate and the slipper.

The force between the slipper and the slipper retainer includes the compression force F_c of the slipper retainer on the slipper, the irregular collision force F_{Her2} between the slipper and the slipper retainer, and the anti-overturning moment M_c applied by the slipper retainer to the slipper. The compression force F_c of the slipper retainer on the slipper is:

$$F_c = kxcos\Upsilon \tag{13}$$

where k is the single spring stiffness, and x is the spring compression amount.

C. MULTI-BODY DYNAMIC MODEL OF AXIAL PISTON PUMP

This article first establishes a 3D model of an axial piston pump in Creo and saves the model in Parasolid (. X_T) file format for importing the 3D model into Adams software. The model only retains the necessary components (drive shaft, swash plate, slipper retainer, slipper, piston, cylinder block, center steel ball) to improve computational efficiency. Motion pairs are added based on the dynamic relationship between components, where the flexible slipper and swash plate are contact pairs. Based on the relevant theories of component flexibility and collision, key parameters in the model are analyzed and set to accurately analyze the overturning and collision behavior of the slipper. Add material properties to each part of the piston pump, and the material parameters are shown in Table 1.

TABLE 1. Material parameter.

Component name	Material	Density(g/mm^3)	Young's modulus(n/mm^2)	Poisson's ratio
Drive shaft	40Cr	7.87×10^{-6}	2.11×10^{5}	0.28
Swash plate	20CrMnTi	7.8×10^{-6}	2.07×10^{5}	0.25
Slipper retainer	38CrMoAlA	7.85×10^{-6}	2.06×10^{5}	0.28
Slipper	QAl9-4	7.5×10^{-6}	1.1×10^{5}	0.33
Piston	GCr15	7.83×10^{-6}	2.19×10^{5}	0.30
Cylinder block	45STELL	7.85×10^{-6}	2.1×10^{5}	0.27
Center steel ball	15CrMo	7.8×10^{-6}	2.04×10^{5}	0.30

The piston pump is the unity of mechanism and fluid. Due to the absence of fluid force in the basic dynamic model, it can only simulate the movement of the piston pump and does not have the function of oil suction and discharge to drive the load. In the previous work [31], we studied the hydraulic pressure characteristics of the piston chamber through a dynamic model of the piston pump. To fully reflect the impact of the piston chamber oil pressure on various components of the piston pump, the oil pressure data obtained from previous research is imported to simulate the process of oil suction and discharge driving the load. Under the piston chamber oil pressure of 343 bar, the load forces of the three adjacent pistons are shown in Fig. 2, while the load force curves of the other six pistons move in phase by 40 degrees in sequence.

According to the working conditions, set the spring force and spring parameters in the spring damping module; To avoid unreasonable force and severe collision of components when the piston pump starts working, a certain acceleration time is added to the drive. After setting the spring and adding the drive, a preliminary multi-body dynamic model can be obtained.

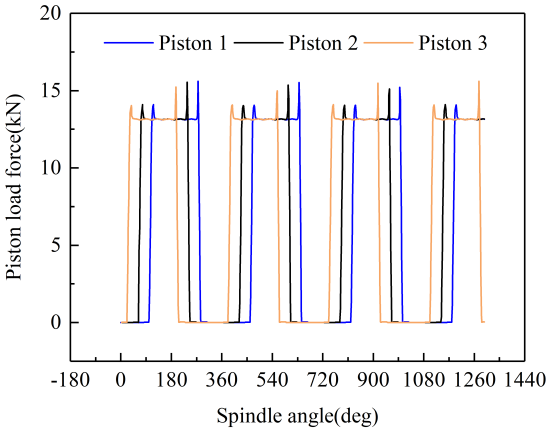

FIGURE 2. Piston load force.

D. RIGID-FLEXIBLE COUPLING MODEL OF THE AXIAL PISTON PUMP

In flexible body dynamics, when a component is considered as a flexible body, the finite element method is generally used to discretize it into a certain number of elements, and the number of elements is positively correlated with the calculation accuracy. The force is transmitted between elements by sharing the same node, resulting in relative displacement between two points on the same element. Then, the stress and strain of the component are further calculated based on the material properties of the element, and the carrier of flexible bodies in multi-body dynamics software is a neutral file containing modal information of components.

As an intermediate link connecting the piston and the swash plate, the force on the slipper is extremely complex, and compared to the couplings of the slipper, the material of the slipper is more prone to wear. Therefore, the slipper is used as a flexible body to observe the stress concentration and deformation of the slipper. Due to the interaction between the slipper and the piston, swash plate, and slipper retainer, there are a total of three rigid areas. Import the modal neutral file generated by Ansys and establish the rigid-flexible coupling model of the piston pump, as shown in Fig. 3.

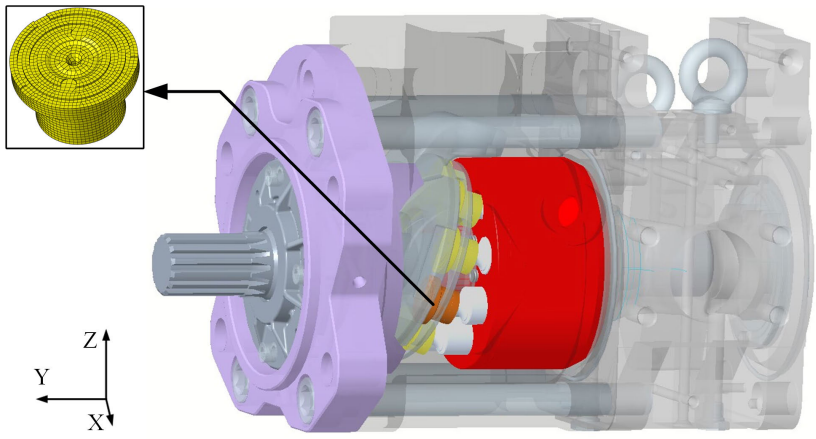

FIGURE 3. Rigid-flexible coupling model of the piston pump.

III. ANALYSIS OF THE OVERTURNING AND COLLISION BEHAVIOR CHARACTERISTICS OF SLIPPERS

This section analyzes the overturning and collision behavior of the slipper under the working condition of 343 bar piston chamber oil pressure and 115 N single spring preload. The five points on the bottom surface of the slipper marked a, b, c, d, and e shown in Fig. 4, are chosen and then the trajectory of each marking is available. The trajectory of the slipper without overturning behavior is regarded as the ideal trajectory, measure the overturning degree of the slipper by the axial distance of the corresponding bottom surface marking point deviating from the ideal trajectory.

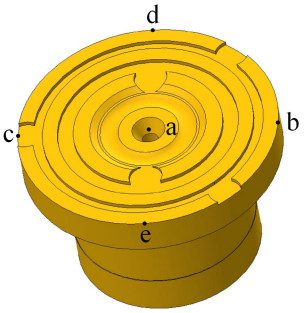

FIGURE 4. The mark point position of the slipper.

Fig. 5 (a) shows the radial positions of each marked point on the slipper (the axial and radial directions mentioned in this article are the axial and radial directions of the spatial coordinates of the piston pump). It can be seen that each marked point is not always in a parallel state, indicating that the slipper exhibits obvious spin behavior during operation; Fig. 5 (b) shows the radial positions of the slipper marking points a and b under 15 N and 115 N single preload conditions. Comparing the radial positions of the slipper marking point b, it is easy to see that the spin speed of the slipper is not consistent under different working conditions. This is caused by the different mechanical characteristics of the slippers and their coupling under different working conditions.

From Fig. 3, it can be seen that the plane between the bottom surface of the slipper and the XZ axis of the piston pump is not consistent. In an ideal working state, the bottom surface of the slipper closely fits the swash plate. Due to the different spin speeds of the slipper under different working conditions, the same marking point will be located in different spatial positions. The micro-motion of spin behavior causes the axial offset distance of the corresponding marking point of the bottom surface of the slipper to constantly change, which cannot reflect the impact of the micro-motion of overturning behavior. The spatial position of the marking point a on the bottom surface of the slipper is not affected by the spin behavior of the slipper. Only when the slipper overturns, its axial coordinates will shift relative to the trajectory without overturning. Therefore, this article uses the axial distance of the marking point a on the bottom surface of the slipper to offset the ideal trajectory as a parameter to measure the overturning degree of the slipper.

Fig. 6 shows the contact force of the slipper/slipper retainer and slipper/swash plate. From Fig. 6, it can be seen that the contact force of the slipper/slipper retainer and slipper/swash plate, exhibits periodicity, which is determined by the oil pressure and flow characteristics of the piston pump. The frequency of curve fluctuation is high, but the contact force does not have a big mutation, indicating that there is a regular collision between the slipper and its coupling, but the fit is relatively stable. Therefore, under this working condition, the slipper has a certain overturning behavior but is not severe, as shown in Fig. 7.

In the working process of the axial piston pump, the piston moves in a reciprocating axial direction within the piston hole, while the slipper follows the piston tightly to fit the surface of the swash plate and performs the high-speed circumferential movement. The centrifugal torque generated by the high-speed circumferential motion of the slipper causes the slipper to have a radial overturning trend, and the frictional

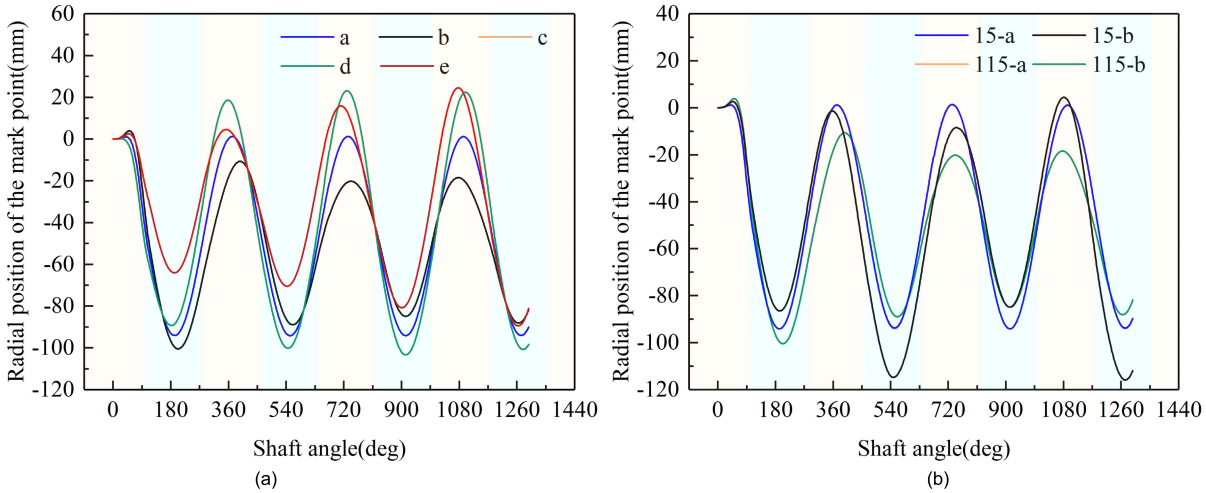

FIGURE 5. Radial position of the mark point: (a) under different position; (b) point a and b under different preloading forces.

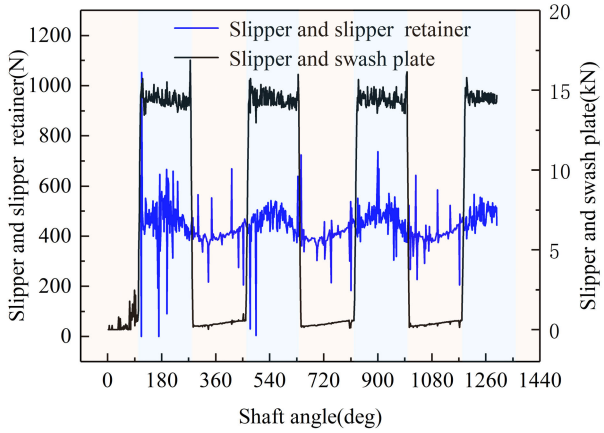

FIGURE 6. Contact force of slipper/slipper retainer and slipper/swash plate.

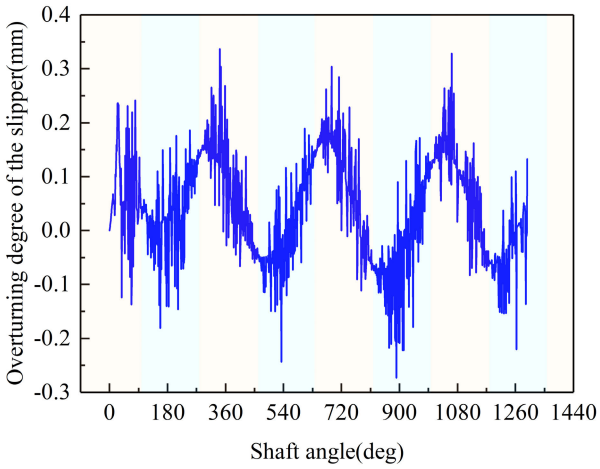

FIGURE 7. Overturning degree of the slipper.

torque generated by the matching between the bottom surface of the slipper and the swash plate causes the slipper to have a circumferential overturning trend. When the working load is complex and variable, or there is no appropriate spring force acting on the slipper retainer, it further exacerbates the overturning behavior of the slipper during periodic operation and also leads to frequent collisions between the slipper and its coupling. The frequent collision between the slipper and its couplings, as well as the overturning behavior of the slipper, will result in uneven oil film thickness on the bottom surface of the slipper, mixed friction, or even dry friction between the bottom surface of the slipper and the swash plate. The friction energy consumption of the piston pump significantly increases, leading to severe partial abrasion of the slipper and even affecting the normal oil suction and discharge process of the axial piston pump. The centrifugal torque generated by the high-speed circumferential movement of the slipper and the friction torque generated by the matching between the bottom surface of the slipper and the swash plate are the fundamental reasons for the overturning and partial abrasion of the slipper. If we want to reduce the overturning degree of the slipper and improve the wear condition, in addition to optimizing the structure of the slipper and its components, we can start from the influence of spring force and piston chamber oil pressure on the overturning and collision behavior of the slipper.

IV. ANALYSIS OF INFLUENCING FACTORS ON SLIPPER OVERTURNING AND COLLISION BEHAVIOR

A. EFFECT OF SPRING PRELOAD ON SLIPPER OVERTURNING AND COLLISION BEHAVIOR

The preload force of the spring is an important factor affecting the overturning and collision behavior of the slipper. In this article, the spring design preload of the piston pump in this article is 1035 N (single spring preload force is 115 N), and the piston chamber oil pressure is 343 bar. In this section, the influence of spring preload on the overturning and collision

behavior of the slipper is studied under the oil pressure of 343 bar.

Fig. 8 shows the overturning degree of the slipper under different spring preloads. It can be seen that the overturning degree of the slipper exhibits a certain periodicity, and the change in spring preload does not affect the period of the overturning behavior of the slipper, which is determined by the oil pressure and flow characteristics of the piston pump. As the preload force of the spring decreases, the overturning degree of the slipper gradually increases. When the preload force of a single spring is less than 30 N, the influence of the preload force on the slipper overturning behavior is more significant. Moreover, when the slipper-piston moves to the oil suction area, the overturning degree of the slipper is the highest, under a single spring preload of 15 N, the maximum overturning degree of the slipper is 1.96 mm; When the slipper-piston moves to the oil discharge area, it is affected by the axial force of the piston and the slipper retainer, and the overturning degree of the slipper is relatively low compared to the oil suction area.

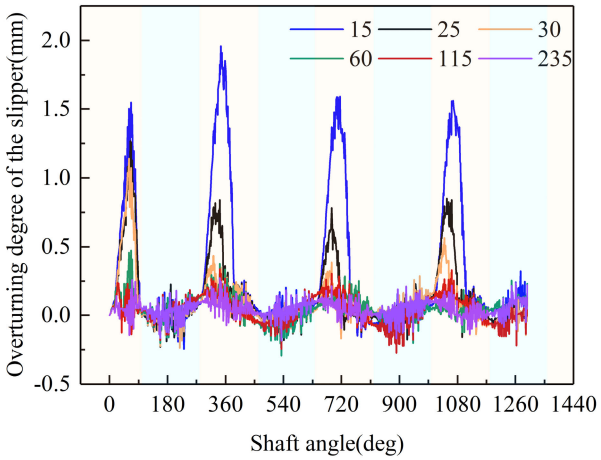

FIGURE 8. Overturning degree of the slipper.

Fig. 9 shows the contact force between the slipper and the slipper retainer under different spring preloads. From Fig. 9, it can be seen that as the spring preload increases, the contact force between the neck of the slipper and the slipper retainer orifice significantly increases. The strong collision between the slipper and the slipper retainer will have an impact on the slipper's attitude. However, at 235 N single spring preload, the contact force between the slipper and the slipper retainer is the highest, and the overturning degree is actually lower. This is because the huge spring force causes the slipper retainer to tightly press the slipper onto the swash plate, reducing the impact of the collision between the slipper and the slipper retainer on the slipper attitude, however, the strong collision between the slipper and the slipper retainer can easily cause fatigue failure of the slipper retainer and excessive wear on the neck of the slipper.

Fig. 10 reflects the effect of spring preload on the contact force between the slipper and the swash plate. It can be

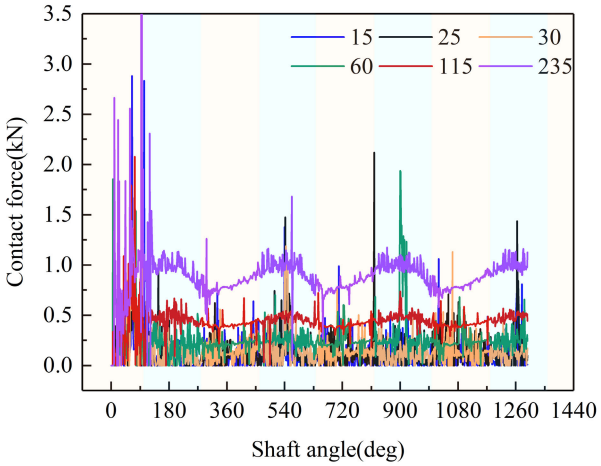

FIGURE 9. Contact force between slipper and slipper retainer.

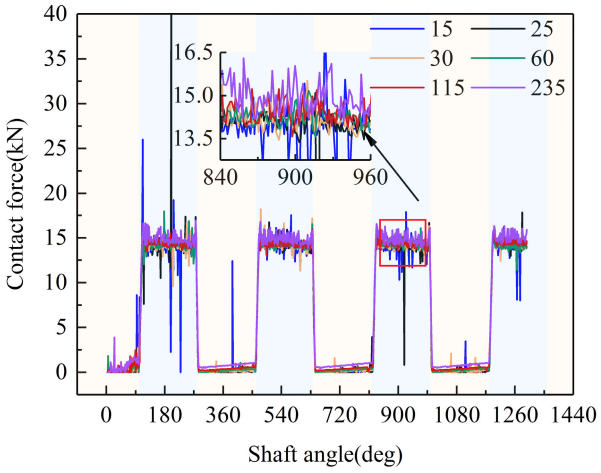

FIGURE 10. Contact force between slipper and swash plate.

seen from Fig. 10 that when the spring preload is low, the fluctuation amplitude of the contact force between the slipper and the swash plate is maximum, and the amplitude change is most significant in the oil discharge area. It is because when the preload force of the spring is low, the overturning behavior of the slipper is more serious, which is more likely to cause a strong collision between the slipper and the swash plate. When the preload force of a single spring is 15 N, the maximum overturning degree of the slipper occurs, and the maximum contact force between the slipper and the swash plate can reach 26000 N, which indicates that there is a strong collision between the slipper and the swash plate. The minimum contact force is close to 0 N, indicating that there is an instantaneous detachment of the bottom surface of the slipper from the contact with the swash plate at this time; As the preload force of the spring increases, the overturning degree of the slipper decreases, and the amplitude of contact force fluctuation between the slipper and the swash plate significantly decreases. The coordination between the

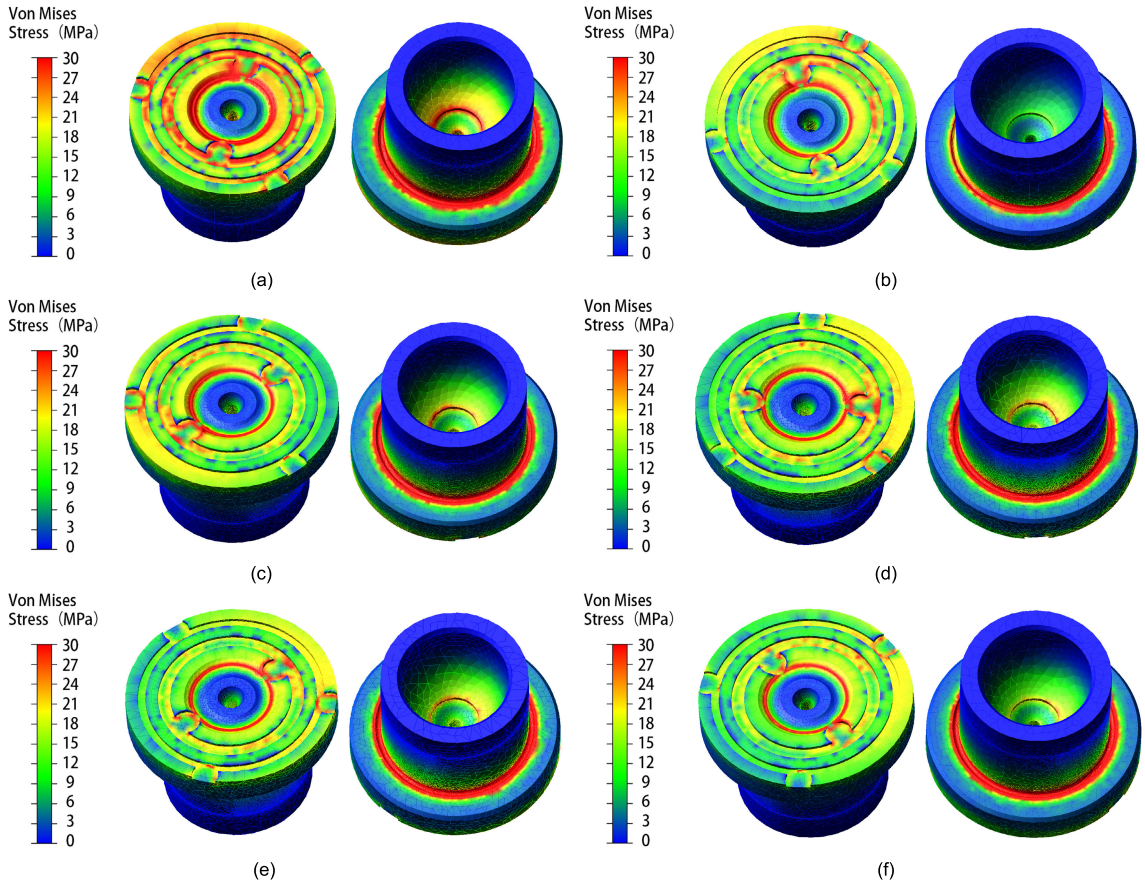

FIGURE 11. Stress nephogram of slipper under different spring preload forces: (a) 15 N; (b) 25 N; (c) 30 N; (d) 60 N; (e) 115 N; (f) 235 N.

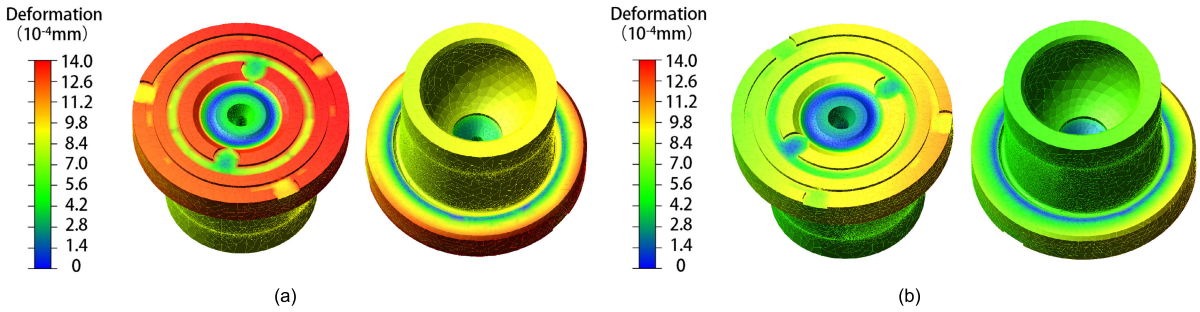

FIGURE 12. Deformation nephogram of slipper under different spring preload force: (a) 15 N; (b) 115 N.

slipper and the swash plate tends to stabilize; When the single spring preload increases to 235 N, compared to the working condition under 115 N single spring preload, the overturning degree of the slipper does not change significantly. Due to the centrifugal torque generated by the circumferential motion of the slipper and the friction torque generated by the matching between the bottom surface of the slipper and the swash plate, there is still a small angle between the bottom surface of the slipper and the swash plate, and the contact force between the slipper and the swash plate shows an increasing trend, as shown in Fig. 10, and the fluctuation amplitude of the contact force between the slipper and the swash plate has increased, indicating that the collision between the slipper and the swashplate is more severe at this time.

To analyze the relationship between the data in more detail, we calculated the mean and standard deviation of the data in Fig. 9 and Fig. 10 in an oil discharge area, and conducted multiple linear regression analysis on the average contact force of the slipper and its coupling and spring preload using SPSS. The regression equation is as follows:

$$F_{pre} = -354.96 + 0.214A + 0.028B \tag{14}$$

Among them, A and B are the average contact force between the slipper and the slipper retainer, and the contact force between the slipper and the swash plate, while F_{pre} is the single spring preload. The regression equation R^2 is greater than 0.95, and the DW value is between 1.5 and 2.5, indicating a high fitting degree of the equation. From Equation 14, it can be seen that the average contact force between the slipper and the slipper retainer, as well as the average contact force between the slipper and the swash plate, is positively correlated with the spring preload. Therefore, as the spring preload increases, the average contact force between the slipper and the slipper retainer increases, and the average contact force between the slipper and the swash plate also increases. When the spring preload is low, the collision strength between the slipper and its coupling has high randomness. For example, the strong collision behavior between the slipper and its coupling may occur in different periods. Therefore, under low preload conditions, there is no significant correlation between the standard deviation of the contact force between the slipper and its coupling and the spring preload; As the spring preload increases, the fit between the slipper and swash plate tends to stabilize, the standard deviation of the contact force between the slipper and the swashplate is positively correlated with the spring preload. Therefore, the fluctuation amplitude of the contact force between the slipper and the swash plate increases with the increase of the spring preload, as shown in Fig. 10.

Therefore, the overturning degree of the slipper can be effectively reduced by increasing the spring preload force, and the collision strength between the slipper and swash plate can be significantly reduced, which can effectively reduce the partial abrasion of the bottom surface of the slipper; But the preload force should not be too large, otherwise, it will cause the thickness of the oil film on the slipper to become thinner, and the collision between the slipper and its coupling will also be more intense, which will exacerbate the wear of the slipper.

In order to further analyze the influence of spring preload on the overturning behavior and mechanical characteristics of the slipper, the stress distribution and deformation at the time corresponding to the maximum stress of the slipper with different preload forces of the spring are analyzed.

For ease of observation, a stress gradient of 0 to 30 MPa and a deformation gradient of 0 to 1.4×10^{-3} mm were selected, it can be seen from Fig. 11 that under a single spring preload of 15 N, the stress distribution of the outer auxiliary support belt of the slipper is extremely uneven. There is severe stress concentration in the oil groove between the sealing belt and the auxiliary support belt, the inner side of the inner auxiliary support belt, and the neck of the slipper. It is because the slipper exhibits obvious overturning behavior under a single spring preload of 15 N. When the slipper-piston transitions from the oil suction area to the oil discharge area, the bottom surface of the slipper collides strongly with the swash plate due to the huge axial force of the piston in the oil discharge area, and the contact force between the slipper and swash plate is as high as 26000 N. The huge contact force not only causes significant stress concentration in the slipper, which also causes large deformation on the auxiliary support belt and sealing belt of the slipper where they contact with the swash plate, as shown in Fig. 12, resulting in partial abrasion on the bottom surface of the slipper.

As the preload force of the spring increases, the overturning degree of the slipper decreases, the collision strength between the slipper and the swash plate decreases, and the stress concentration area and maximum stress on the bottom surface of the slipper significantly decrease, as shown in Figs. 11 and 13, and the partial abrasion of the slipper is significantly alleviated; When the preload is 115 N, the stress concentration area on the bottom surface and neck of the slipper is the smallest and the stress distribution is the best. In this working condition, the overturning degree of the slipper is relatively small, and the maximum contact force between the slipper and the swash plate is 16879 N, which is much lower than the working condition when the single spring preload is 15 N; When the preload increases to 235 N, the stress concentration area and maximum stress at the bottom surface and neck of the slipper tend to increase, and the fluctuation amplitude of the contact force between the slipper and the swash plate increases under this working condition, and the collision between the slipper and the slipper retainer becomes more intense.

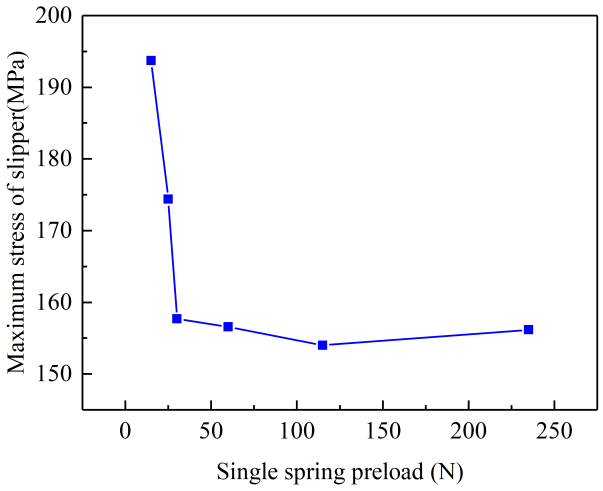

FIGURE 13. Maximum stress of slipper.

In addition, due to the overturning behavior of the slipper, the collision between the piston and the slipper is more intense. Under the large axial force of the piston in the oil discharge area, the ball socket of the slipper undergoes large deformation. Therefore, the deformation of the slipper ball socket under the 15 N single spring preload is larger than that under the 115 N single spring preload condition, as shown in Fig. 12. Besides, the stress concentration in the neck of the slipper is more pronounced with a single spring preload of 15 N. At this time, the stress in the neck of the slipper reaches a maximum of 193 MPa. However, at a single spring preload of 115 N, the slipper works more stably without

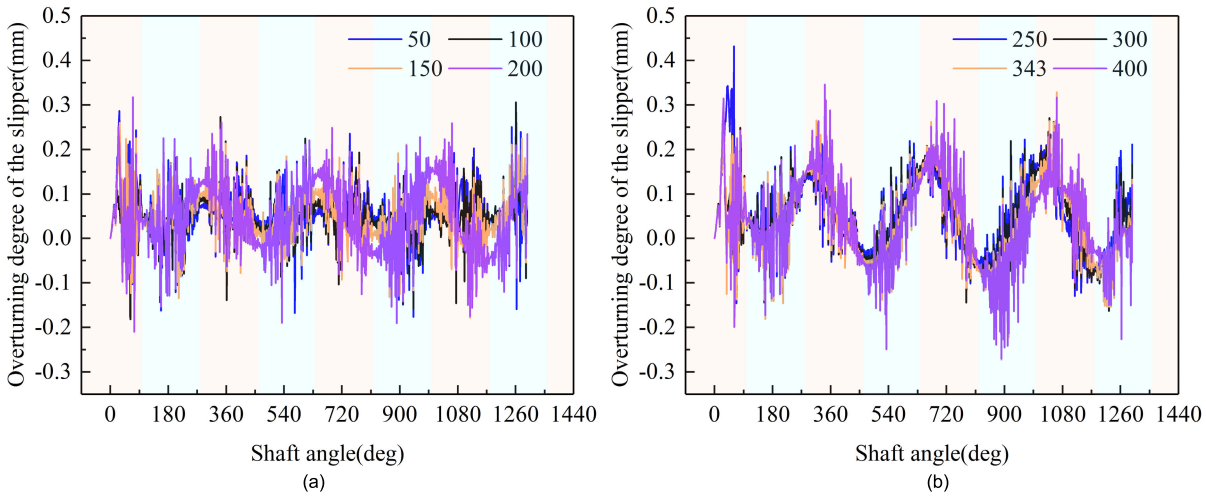

FIGURE 14. Overturning degree of the slipper: (a) and (b) under different piston chamber oil pressure.

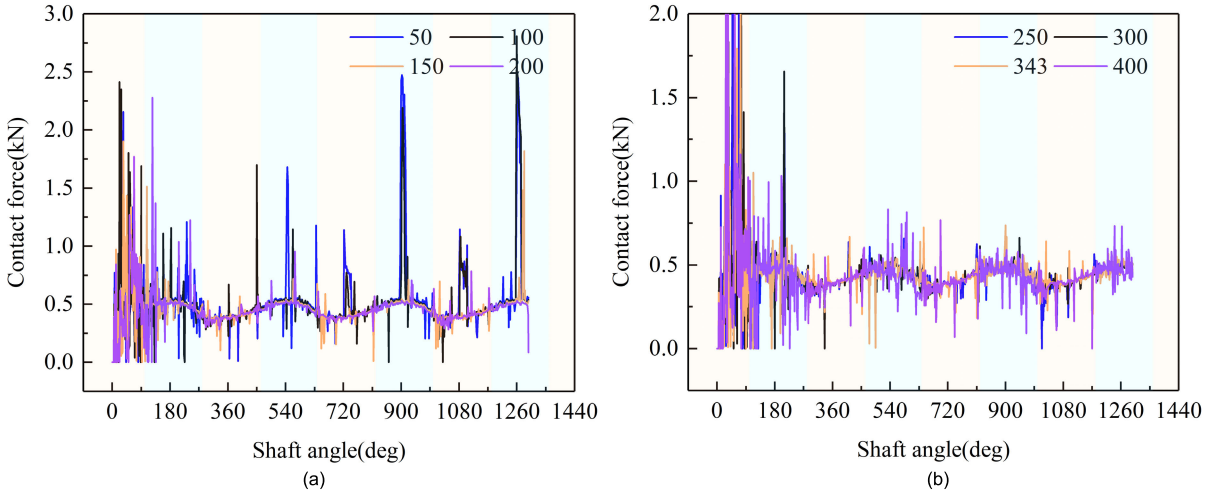

FIGURE 15. Contact force between slipper and slipper retainer: (a) and (b) under different piston chamber oil pressure.

strong collision with the swash plate, and the stress in the neck reaches a maximum of 154 MPa. Except for the obvious stress concentration in the neck of the slipper and the oil groove at the inner side of the inner auxiliary support belt, the stress and deformation in other positions are relatively even.

B. EFFECT OF PISTON CHAMBER OIL PRESSURE ON SLIPPER OVERTURNING AND COLLISION BEHAVIOR

The piston chamber oil pressure is an important factor affecting the overturning and collision behavior of the slipper. In this section, the influence of piston chamber oil pressure on the overturning and collision behavior of the slipper is studied under a 1035 N spring preload.

Fig. 14 shows the overturning degree of the slipper under different piston chamber oil pressure. It can be seen that the overturning degree of the slipper exhibits a certain periodicity, and the change in piston chamber oil pressure does not affect the period of slipper overturning, which is determined by the oil pressure and flow characteristics of the piston pump. As the piston chamber oil pressure increases, the overturning degree of the slipper tends to increase, and the slipper overturning behavior is most severe when the slipper-piston transitions from the oil discharge area to the oil suction area. The reason is that the oil has compressibility, the piston chamber oil in the oil discharge area is in a state of high pressure, and the oil has a large elastic potential energy. When the slipper-piston translates from the oil discharge area to the oil suction area, the sudden change of flow and the instantaneous release of elastic potential energy will easily lead to a collision between the slipper and the swash plate, and then the bottom surface of the slipper cannot cling to the swash plate. At the same time, the slipper will overturn under the influence of centrifugal torque and friction torque.

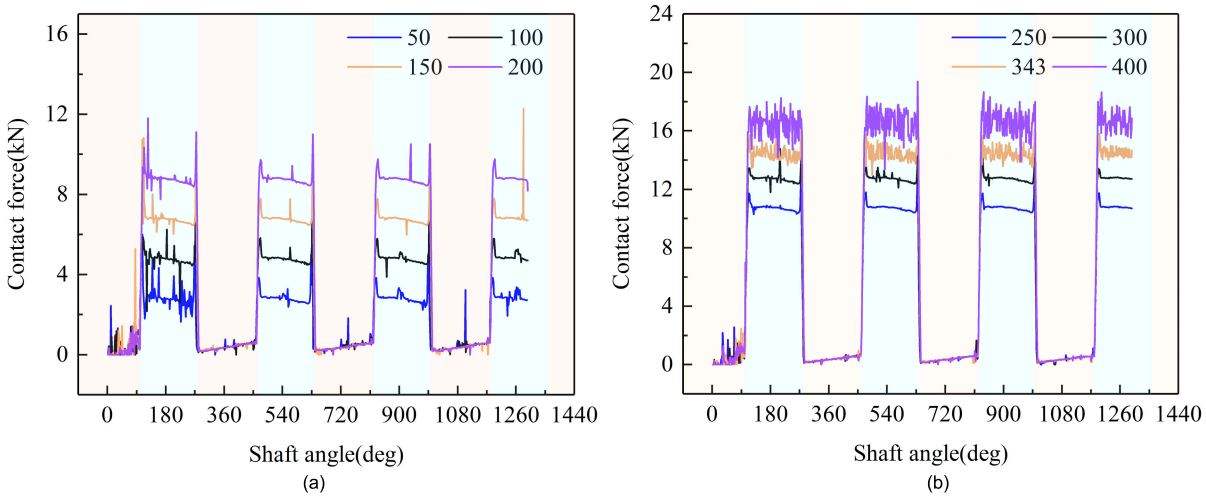

FIGURE 16. Contact force between slipper and swash plate: (a) and (b) under different piston chamber oil pressure.

Fig. 15 shows the contact force between the slipper and the slipper retainer under different piston chamber oil pressure. From Fig. 15, it can be seen that as the piston chamber oil pressure increases, there is no significant change in the trend of the contact force between the slipper and the slipper retainer, while there is a certain change in the fluctuation amplitude of the contact force, at the turning point of the 250 bar piston chamber oil pressure, the fluctuation amplitude of the contact force between the slipper and the slipper retainer shows a pattern of first decreasing and then increasing. This is because under higher piston chamber oil pressure, the degree of slipper overturning is greater, resulting in more frequent collisions between the slipper and the slipper retainer. However, the increase in piston chamber oil pressure does not directly affect the magnitude of the axial force between the slipper and the slipper retainer, therefore, there is a phenomenon where the contact force between the slipper and the slipper retainer does not increase with the fluctuation amplitude.

Fig. 16 reflects the effect of piston chamber oil pressure on the contact force between the slipper and the swash plate. From Fig. 16, it can be seen that as the piston chamber oil pressure increases, the contact force between the slipper and the swash plate in the oil discharge area increases, and at the same time, the fluctuation amplitude of the contact force between the slipper and the swash plate also significantly increases. It is because as the piston chamber oil pressure increases, the overturning degree of the slipper increases, and the fit between the slipper and the swash plate tends to be unstable. The collision between the slipper and the swash plate occurs frequently and becomes more severe, thereby exacerbating partial abrasion on the bottom surface of the slipper.

To analyze the relationship between the data in more detail, we calculated the average value and standard deviation of the data in Fig. 15 and Fig. 16 in an oil discharge area, and conducted multiple linear regression analysis on the average contact force between the slipper and its couplings and the piston chamber oil pressure using SPSS, as well as the standard deviation of the contact force and the piston chamber oil pressure. The regression equation is as follows:

$$F_{oil1} = -34.884 + 0.019A + 0.028B \tag{15}$$

$$F_{oil2} = -24.635 - 0.028C + 0.102D \tag{16}$$

Among them, C and D are the standard deviations of the contact force between the slipper and the slipper retainer and the contact force between the slipper and the swash plate, and F_{oil} is the piston chamber oil pressure. The regression equations R^2 are all greater than 0.95, the VIF values are all less than 4, and the DW values are 1.817 and 2.887, indicating a high degree of equation fitting. From Equation 15, it can be seen that the average contact force between the slipper and the slipper retainer, as well as the average contact force between the slipper and the swash plate, are positively correlated with the piston chamber oil pressure. Therefore, as the piston chamber oil pressure increases, the average contact force between the slipper and the slipper retainer increases, and the average contact force between the slipper and the swash plate also increases. From Equation 16, it can be seen that the standard deviation of the contact force between the slipper and the swash plate is positively correlated with the piston chamber oil pressure. Therefore, as the piston chamber oil pressure increases, the standard deviation of the contact force between the slipper and the swash plate increases, which means that the fluctuation amplitude of the contact force between the slipper and the swash plate increases; The standard deviation of the contact force between the slipper and the slipper retainer is negatively correlated with the piston chamber oil pressure. As the piston chamber oil pressure increases, the calculated standard deviation of the contact force between the slipper and the slipper retainer

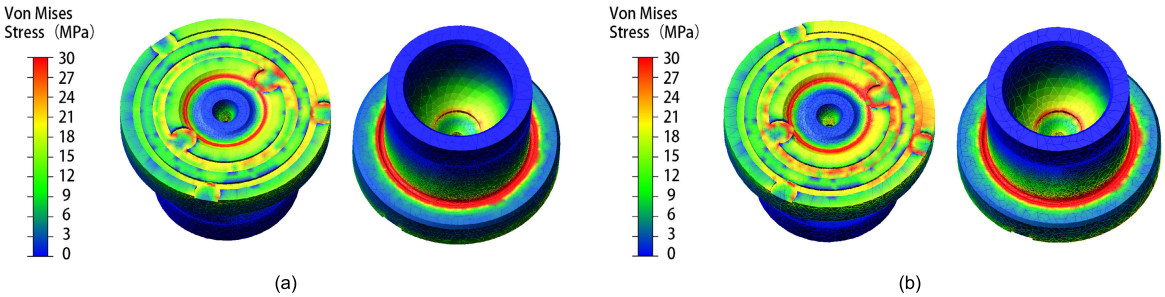

FIGURE 17. Stress nephogram of slipper under different piston chamber oil pressure: (a) 343 bar; (b) 400 bar.

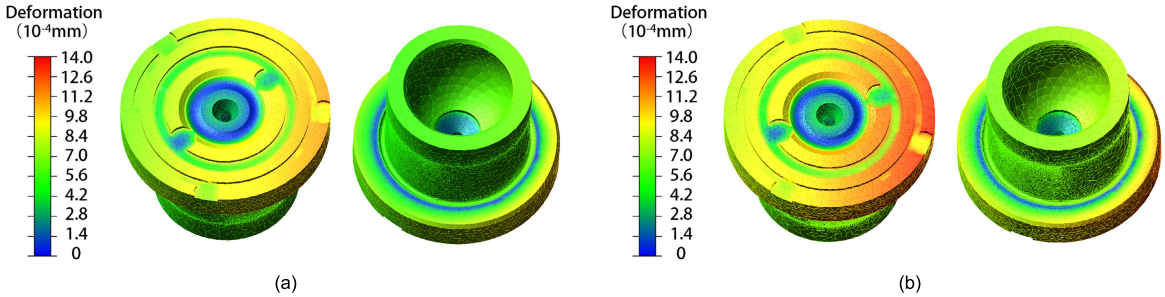

FIGURE 18. Deformation nephogram of slipper under different piston chamber oil pressure: (a) 343 bar; (b) 400 bar.

decreases first and then increases. This is because, in the regression analysis of Equation 16, the *DW* value is 2.887, greater than 2.5, indicating a certain degree of autocorrelation between variables, which affects the accuracy of the correlation between each variable, however, for the values of each variable, Equation 16 still has a good fitting effect.

Due to the maximum overturning degree of the slipper under the working conditions of 343 bar and 400 bar oil pressure, and the most unstable matching between the slipper and its coupling, in order to further analyze the influence of piston chamber oil pressure on the overturning behavior and mechanical characteristics of the slipper, the stress distribution and deformation at the time corresponding to the maximum stress of the slipper under the oil pressure of 343 bar and 400 bar piston chamber are analyzed.

For ease of observation, a stress gradient of 0 to 30 MPa and a deformation gradient of 0 to 1.4×10^{-3} mm were selected. As shown in Fig. 17, under the piston chamber oil pressure of 343 bar, the stress distribution of the outer auxiliary support belt of the slipper is uneven. There is a significant stress concentration on the inner side of the inner auxiliary support belt and the neck of the slipper. When the piston chamber oil pressure increases to 400 bar, the position of the stress concentration does not change significantly, and the stress value and area of the stress concentration increase. This is because as the piston chamber oil pressure increases, The axial force transmitted by the piston to the slipper further increases, while the overturning degree of the slipper increases. When the slipper piston translates from the oil discharge area to the oil suction area, the collision between the slipper and the swash plate becomes more severe, and the fluctuation amplitude and frequency of the contact force between the slipper and the swash plate increase significantly. The stress concentration on the bottom surface of the slipper is more significant, which also causes large deformation on the auxiliary support belt and sealing belt of the slipper where they contact with the swash plate, As shown in Fig. 18. This can lead to partial abrasion of the outer auxiliary support belt and sealing belt on the bottom surface of the slipper.

In addition, as the piston chamber oil pressure increases and is affected by the overturning behavior of the slipper, the collision between the slipper and the piston becomes stronger, and the deformation of the ball socket of the slipper is more obvious. The stress concentration in the neck of the slipper is more significant, and the maximum stress in the neck of the slipper is 177.49 MPa at this time.

V. CONCLUSION

Based on the nonlinear finite element contact collision theory, the rigid-flexible coupling dynamics model of the swash plate axial piston pump is established in this article. Under the consideration of friction torque, inertia torque and component flexibility and other factors, the collision relationship between the slipper and its coupling, the overturning behavior characteristics of the slipper, and the change law of the overturning and collision behavior of the slipper under different spring forces and piston chamber oil pressure were studied by simulation. The stress distribution and deformation of the slipper under different working conditions were also studied. The research found that:

(1) In the marking points on the bottom surface of the slipper, point a is not affected by the self-spin behavior of the slipper, and the axial distance of point a deviating from the ideal trajectory is taken as the parameter to measure the overturning degree of the slipper. Under reasonable working parameters, the slipper has a certain overturning behavior due to the influence of centrifugal moment generated by its circumferential movement and friction moment generated by matching with the swash plate. The overturning behavior of the slipper is periodic, and the maximum overturning degree is located in the oil suction area. There is a regular collision between the slipper and its coupling, but the cooperation is relatively stable.

(2) Increasing the preload force of the spring appropriately can reduce the overturning degree of the slipper, and the matching between the slipper and the slipper coupling will be more stable, which can effectively reduce partial abrasion on the bottom surface of the slipper; However, the preload should not be too high, otherwise it will cause the thickness of the oil film of the slipper/swash plate pair to become thinner, at the same time, the average contact force between the slipper and the slipper retainer, as well as the contact force between the slipper and the swash plate increases, resulting in stronger collision between the slipper and its coupling, thereby accelerating the wear of the bottom surface of the slipper. Under the working condition of a large overturning degree of the slipper, the stress distribution of the outer auxiliary support belt of the slipper is extremely uneven. There is significant stress concentration in the oil groove between the sealing belt of the slipper and the auxiliary support belt, the inner side of the inner auxiliary support belt, and the neck of the slipper. At the same time, there is significant deformation on the auxiliary support belt and sealing belt of the slipper where they contact with the swash plate, leading to partial abrasion on the bottom surface of the slipper.

(3) As the piston chamber oil pressure increases, the overturning degree of the slipper tends to increase, and when the slipper-piston translates from the oil discharge area to the oil suction area, the overturning behavior of the slipper is the most severe. As the piston chamber oil pressure increases, the average contact force between the slipper and the swash plate increases, while the average contact force between the slipper and the slipper retainer decreases, at the turning point of the 250 bar piston chamber oil pressure, the fluctuation amplitude of the contact force between the slipper and the slipper retainer shows a pattern of first decreasing and then increasing, besides, the standard deviation of the contact force between the slipper and the swash plate continues to increase, indicating that the collision between the slipper and its coupling is more frequent and severe under high pressure, exacerbating the wear of the slipper.

The existing experiments on the overturning behavior of slippers have undergone many simplifications. Without neglecting the collision behavior between the slipper and its coupling, the measurement of the overturning degree of the slipper is relatively difficult for the current experimental conditions, which needs to be further improved in future work. The research results of this article provide a reference for the wear failure analysis and structural optimization of the slipper.

REFERENCES

[1] H. Tang, Z. Fu, and Y. Huang, "A fault diagnosis method for loose slipper failure of piston pump in construction machinery under changing load," *Appl. Acoust.*, vol. 172, Jan. 2021, Art. no. 107634, doi: 10.1016/j.apacoust.2020.107634.

[2] Y. Lan, Z. Li, S. Liu, J. Huang, L. Niu, X. Xiong, C. Niu, B. Wu, X. Zhou, J. Yan, S. An, and J. Lv, "Experimental investigation on cavitation and cavitation detection of axial piston pump based on MLP-mixer," *Measurement*, vol. 200, Aug. 2022, Art. no. 111582.

[3] H. C. Wu and Y. L. Yu, "Study on the influence of deformation of the slipper of axial piston pump under high pressure on oil film structure," in *Proc. Int. Forum Mater. Process. Technol.*, Guangzhou, China, 2014, pp. 734–737, doi: 10.4028/www.scientific.net/AMR.900.734.

[4] X. Zhang, H. Wu, C. Chen, D. Wang, and S. Li, "Oil film lubrication state analysis of piston pair in piston pump based on coupling characteristics of the fluid thermal structure," *Eng. Failure Anal.*, vol. 140, Oct. 2022, Art. no. 106521, doi: 10.1016/j.engfailanal.2022.106521.

[5] J.-H. Shin, "Computational study on dynamic pressure in a swash-plate axial piston pump connected to a hydraulic line with an end resistance," *J. Mech. Sci. Technol.*, vol. 29, no. 6, pp. 2381–2390, Jun. 2015, doi: 10.1007/s12206-015-0531-1.

[6] S. Liu, Y. Zhang, C. Ai, Y. Ge, Z. Li, Y. Zhu, and M. Hao, "A new test method for simulating wear failure of hydraulic pump slipper pair under high-speed and high-pressure conditions," *Frontiers Energy Res.*, vol. 10, pp. 1–12, Jan. 2023, doi: 10.3389/fenrg.2022.1096633.

[7] J. Zhang, Q. Chao, B. Xu, M. Pan, Y. Chen, Q. Wang, and Y. Li, "Effect of piston-slipper assembly mass difference on the cylinder block tilt in a high-speed electro-hydrostatic actuator pump of aircraft," *Int. J. Precis. Eng. Manuf.*, vol. 18, no. 7, pp. 995–1003, Jul. 2017, doi: 10.1007/s12541-017-0117-1.

[8] R. Gupta, A. Miglani, and P. K. Kankar, "Performance prediction of an axial piston pump with increasing severity of leakage fault in single and multiple cylinders," *J. Dyn. Syst., Meas., Control*, vol. 145, no. 2, Feb. 2023, doi: 10.1115/1.4056026.

[9] H. Wu, L. Zhao, S. Ni, and Y. He, "Study on friction performance and mechanism of slipper pair under different paired materials in high-pressure axial piston pump," *Friction*, vol. 8, no. 5, pp. 957–969, Oct. 2020, doi: 10.1007/s40544-019-0314-2.

[10] R. M. Harris, K. A. Edge, and D. G. Tilley, "Predicting the behavior of slipper pads in swashplate-type axial piston pumps," *J. Dyn. Syst., Meas., Control*, vol. 118, no. 1, pp. 41–47, Mar. 1996.

[11] L. Hu, H. Wu, L. Zhao, and S. Ni, "Development of electro—Hydraulic control platform for high speed slipper pair friction test machine," in *Proc. 2nd Int. Symp. Resource Explor. Environ. Sci.*, 2018, pp. 1–12, doi: 10.1088/1755-1315/170/4/042128.

[12] Y. Lan, J. Hu, J. Huang, L. Niu, X. Zeng, X. Xiong, and B. Wu, "Fault diagnosis on slipper abrasion of axial piston pump based on extreme learning machine," *Measurement*, vol. 124, pp. 378–385, Aug. 2018, doi: 10.1016/j.measurement.2018.03.050.

[13] J. Zhang, Q. Chao, Q. Wang, B. Xu, Y. Chen, and Y. Li, "Experimental investigations of the slipper spin in an axial piston pump," *Measurement*, vol. 102, pp. 112–120, May 2017, doi: 10.1016/j.measurement.2017.01.035.

[14] T. Ransegnola, L. Shang, and A. Vacca, "A study of piston and slipper spin in swashplate type axial piston machines," *Tribol. Int.*, vol. 167, Mar. 2022, Art. no. 107420, doi: 10.1016/j.triboint.2021.107420.

[15] J. Zhou, J. Zhou, and C. Jing, "Experimental research on the dynamic lubricating performance of slipper/swash plate interface in axial piston pumps," *Chin. J. Mech. Eng.*, vol. 33, no. 1, pp. 1–20, Dec. 2020, doi: 10.1186/s10033-020-00441-7.

[16] B. Xu, J. Zhang, and H. Yang, "Investigation on structural optimization of anti-overturning slipper of axial piston pump," *Sci. China Technol. Sci.*, vol. 55, no. 11, pp. 3010–3018, Nov. 2012, doi: 10.1007/s11431-012-4955-x.

[17] Q. Chao, J. Zhang, B. Xu, Q. Wang, F. Lyu, and K. Li, "Integrated slipper retainer mechanism to eliminate slipper wear in high-speed axial piston pumps," *Frontiers Mech. Eng.*, vol. 17, no. 1, pp. 1–12, Mar. 2022.

[18] J. Jiang and Z. Wang, "Optimization and influence of micro-chamfering on oil film lubrication characteristics of slipper/swashplate interface within axial piston pump," *Energies*, vol. 14, no. 7, p. 1961, Apr. 2021, doi: 10.3390/en14071961.
[19] X. Meng, C. Ge, H. Liang, X. Lu, and X. Ma, "Lubrication characteristics of the slipper-swash-plate interface in a swash-plate-type axial piston pump," *Proc. Inst. Mech. Eng., C, J. Mech. Eng. Sci.*, vol. 235, pp. 639–651, Jan. 2021.
[20] Ö. Özmen, C. Sinanoğlu, A. Caliskan, and H. Badem, "Prediction of leakage from an axial piston pump slipper with circular dimples using deep neural networks," *Chin. J. Mech. Eng.*, vol. 33, no. 1, pp. 1–16, Dec. 2020, doi: 10.1186/s10033-020-00443-5.
[21] A. Shorbagy, R. Ivantysyn, and J. Weber, "Holistic analysis of the tribological interfaces of an axial piston pump—Focusing on the pump efficiency," *Chem. Eng. Technol.*, vol. 46, no. 1, pp. 5–13, Jan. 2023, doi: 10.1002/ceat.202200450.
[22] H. Tang, Y. Ren, and J. Xiang, "A novel model for predicting thermoelastohydrodynamic lubrication characteristics of slipper pair in axial piston pump," *Int. J. Mech. Sci.*, vols. 124–125, pp. 109–121, May 2017, doi: 10.1016/j.ijmecsci.2017.03.010.
[23] T. Hesheng, Y. Yaobao, and L. Jing, "Lubrication characteristics analysis of slipper bearing in axial piston pump considering thermal effect," *Lubrication Sci.*, vol. 28, no. 2, pp. 107–124, Mar. 2016, doi: 10.1002/ls.1304.
[24] L. Wang, M. Hu, Y. Zeng, S. Shong, C. Liu, and R. Liu, "Relative motion relationship and collision mechanism of slipper-retainer assembly of axial piston machines," *Proc. Inst. Mech. Eng., C, J. Mech. Eng. Sci.*, vol. 237, no. 6, pp. 1323–1343, Mar. 2023, doi: 10.1177/09544062221132116.
[25] G. Haidak and D. Wang, "Research on the thermo-elastic deformation and fracture mechanism of the slipper retainer in the axial piston pumps and motors," *Eng. Failure Anal.*, vol. 100, pp. 259–272, Jun. 2019, doi: 10.1016/j.engfailanal.2019.02.041.
[26] M. Hu, B. Xu, W. Zhou, and S. Xia, "Modelling and analysis of dynamics characteristics of piston-slipper group of axial piston pump," *Trans. Chin. Soc. Agricult. Machinery*, vol. 47, no. 3, pp. 373–380, 2016, doi: 10.6041/j.issn.1000-1298.2016.03.053.
[27] M. Decken and H. Murrenhoff, "Simulation of fluid power components using DSHplus and ADAMS," in *Proc. ASME Int. Mech. Eng. Congr. Expo.*, New York, NY, USA, Nov. 2001, pp. 2559–2565.
[28] H. Shen, Z. Zhou, D. Guan, Z. Liu, L. Jing, and C. Zhang, "Dynamic contact analysis of the piston and slipper pair in axial piston pump," *Coatings*, vol. 10, no. 12, p. 1217, Dec. 2020, doi: 10.3390/coatings10121217.
[29] L. Yang, H. Li, Y. Li, and K. Dang, "Bearing characteristics analysis and multi-field coupling simulation on slipper-piston component," in *Proc. IEEE 11th Conf. Ind. Electron. Appl. (ICIEA)*, Jun. 2016, pp. 2462–2467, doi: 10.1109/ICIEA.2016.7604006.
[30] Y. Yao, A. Z. Qamhiyah, and X. D. Fang, "Finite element analysis of the crimping process of the piston-slipper component in hydraulic pumps," *J. Mech. Des.*, vol. 122, no. 3, pp. 337–342, Sep. 2000, doi: 10.1115/1.1286188.
[31] Z. Sun, Q. Zeng, L. Wan, and H. Dai, "Control and dynamic characteristics analysis for the double-compound axial piston pump based on working conditions," *Machines*, vol. 10, no. 6, p. 411, May 2022, doi: 10.3390/machines10060411.

LIRONG WAN received the Ph.D. degree from the Shandong University of Science and Technology, in 2008. She is currently a Professor with the Shandong University of Science and Technology. Her research interests include hydraulic transmission and control, mechatronics, computer-integrated manufacturing, and virtual prototype.

JINYING JIANG was born in 1999. He received the B.E. degree in mechanical and electronic engineering from the Shandong University of Science and Technology, in 2021, where he is currently pursuing the M.E. degree. His research interests include transmission and control of hydraulic systems, and mechatronics integration.

ZHIYUAN SUN is currently pursuing the Ph.D. degree with the Shandong University of Science and Technology, China. His research interests include fluid power transmission and control and mechatronics.

HAO NIU was born in 1999. He received the B.E. degree in mechanical and electronic engineering from the Shandong University of Science and Technology, Qingdao, China, in 2021. His research interests include transmission, epicyclic gear train, and gear churning oil loss.